STM Study of Multiple Bonding Configurations and Mechanism of 1,3-Cyclohexadiene Attachment on Si(100)-2 × 1

Lucile C. Teague and John J. Boland*

Venable and Kenan Laboratories, Department of Chemistry, University of North Carolina at Chapel Hill, Chapel Hill, North Carolina 27599

Received: December 5, 2002; In Final Form: February 20, 2003

Scanning tunneling microscopy (STM) was used to investigate the reaction of 1,3-cyclohexadiene with Si dimers on the bare Si(100) surface. Detailed, high-resolution STM images show a distribution of surface products. In addition to the intradimer [2 + 2] and [4 + 2] reaction products previously reported, two different [2 + 2] conformers are identified. Empty state STM images also show interdimer [4 + 2] reactions involving neighboring dimers in the same row and in adjacent rows. The former are shown to be the dominant surface product despite the presence of unpaired dangling bonds on two adjacent dimers. These results are interpreted in terms of a reaction mechanism in which the reduced ring strain favors the kinetic interdimer [4 + 2] product over the thermodynamically stable [4 + 2] intradimer product.

Introduction

Covalent attachment of organic molecules to semiconductor surfaces has been the focus of several recent experimental[1−6] and theoretical[7,8] studies. The ability to design and attach organic layers of controlled thicknesses and functionalities opens up potential applications in the areas of nanoscale devices.[9] In principle, molecules can serve as both passive and active components in nanoscale devices, ranging from ultrathin insulating spacer layers to molecular switches. However, before such devices can be realized, it is necessary to have a full understanding of how molecules attach and organize themselves on substrates. In particular, it is necessary to develop methods that distinguish between and indeed identify different modes of molecular attachment. Since conventional devices are silicon based, there has been significant, recent interest in attachment chemistries involving silicon surfaces, especially the Si(100) surface.

Recent STM studies have reported the attachment of a wide variety of organic molecules to Si(100).[1,2,4−6] In many instances, however, it has proven difficult to achieve adequate resolution to allow discrimination between different products. Here in this report, we describe the attachment of 1,3-cyclohexadiene (1,3-CHD) to the Si(100)-2 × 1 surface. This system was chosen because of the possibility of a broad range of products, which allows us to push the limits of attainable resolution and to explore the ground rules for molecular attachment on Si(100). Since dimers on the Si(100) surface have significant π character, cycloadditon reactions with molecules such as 1,3-CHD can be classified as being either [4 + 2]- or [2 + 2]-like. This expectation is consistent with the earliest filled state study of the 1,3-CHD exposed Si(100) surface, which revealed the presence of two dominant kinds of molecular adducts.[1] In their pioneering work, Hovis et al. identified these species as the [2 + 2] and [4 + 2] adducts, with the latter being the dominant product. More recent theoretical studies[8] have also suggested the possibility of two kinds of [2 + 2] conformers. However, all experimental and theoretical studies to date have focused on reaction involving single Si(100) dimer units. Here, in this present work, we provide a high-resolution STM study of the reaction of 1,3-CHD with Si(100). We unambiguously identify five different surface reaction products, including two different [2 + 2] conformers and two different interdimer [4 + 2] products. The aforementioned STM study by Hovis et al. identified the [2 + 2] and [4 + 2] reaction products based on filled-state STM images. However, in the present study, in addition to [2 + 2] and [4 + 2] products, we identify new reaction products, including those that involve reaction with more than one dimer unit. Identification of the complete product distribution is possible only in empty state images and is due to an ability to locate the single remaining π bonds in the molecular adducts under these bias conditions. We discuss these results in terms of a reaction mechanism in which ring strain plays a pivotal role in determining the product distribution.

Experimental Section

All experiments were performed in an Omicron variable temperature STM (VT-STM) with a base pressure of ∼5 × 10^{-11} Torr. The Si(100)-2 × 1 samples were cut from phosphorus-doped n-type Si(100) wafers (1 Ω·cm). They were initially outgassed by indirect heating, then flashed to ∼1350 K and slowly cooled to room temperature to yield a clean 2 × 1 surface. 1,3-CHD (>97% purity) was obtained from Aldrich. The molecule was first degassed with Ar, dried over molecular sieves, and then transferred to a vacuum ampule in a glovebox. Several freeze−pump−thaw cycles were then performed as the last step in purification of the compound. 1,3-CHD was introduced directly into the STM chamber via a variable leak valve, and the dose was determined by monitoring the chamber pressure using an ion-gauge. A typical dose was ∼3 × 10^{-10} Torr (uncorrected for the reduced sensitivity to 1,3-CHD) for 5 s at room temperature. Images were recorded over a range of current and bias conditions. The results reported here have been observed with numerous Si substrates, tips, and different sources of 1,3-CHD.

* To whom correspondence should be addressed. Present address: Department of Chemistry, Trinity College, Dublin 2, Ireland. E-mail: jboland@tcd.ie.

10.1021/jp027632n CCC: $25.00
Published on Web 04/01/2003

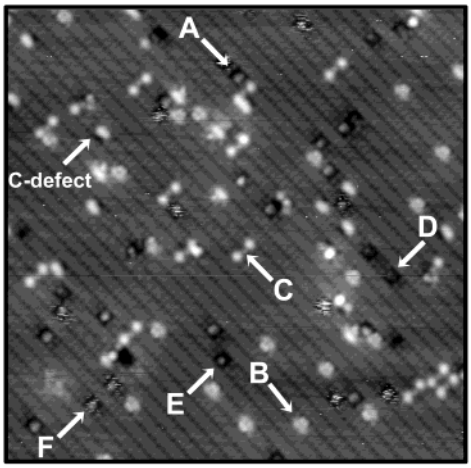

Figure 1. STM image (25 nm × 25 nm, $V_{tip} = -1.3$ V) of Si(100) surface following 300 K submonolayer exposure to 1,3-cyclohexadiene. Arrows A−F indicate the different molecule derived species on the surface.

Results and Discussion

Figure 1 shows an empty state image (−1.3 V tip bias) of the Si(100) surface following a 300 K submonolayer exposure to 1,3-CHD. A broad product distribution is immediately evident. The arrows (A−F) identify six different molecule-derived features found on the surface. These features can be clearly distinguished from the missing dimer and C-defects known to exist on this surface.[10] High-resolution empty state images of these species are shown in Figure 2. Each species is imaged as a shallow depression, i.e., a region of reduced tunneling current, which contains one or two well-defined maxima. MIR-FTIR and NEXAFS studies[11] confirm that 1,3-CHD molecules undergo cycloaddition reactions with the Si-(100) dimers, and in each case, a single intact C═C remains in the molecular adduct. Since this remaining π state is closer to the Fermi energy than the σ bonded skeleton,[11] it is reasonable to assign the bright maxima in Figure 2 to the C═C in the molecule. Moreover, since the orientation of the C═C bond depends on the attachment chemistry, the registry of the maxima with respect to the underlying Si dimer row provides a means of product identification. In following paragraphs, we detail how this method can be used to identify the reaction products in the present system.

In addition to high-resolution STM images, Figure 2 also shows ball-and-stick models that illustrate the attachment of the molecule to the underlying surface. These models have been relaxed so that the structure shown reflects the actual geometry of the product.[12] On this basis, products A−C are identified as [4 + 2]-like cycloaddition products. Based on its orientation, A is assigned to be the intradimer [4 + 2] product. It has a two-dimer footprint, similar to that reported for other adsorbates such as acetylene[13] and 1,4-cyclohexadiene.[14] It consists of an oblong shaped maximum located to one end of the darker footprint and exhibits a clearly discernible node that is ascribed to the remaining π bond in the [4 + 2] adduct. Comparison of

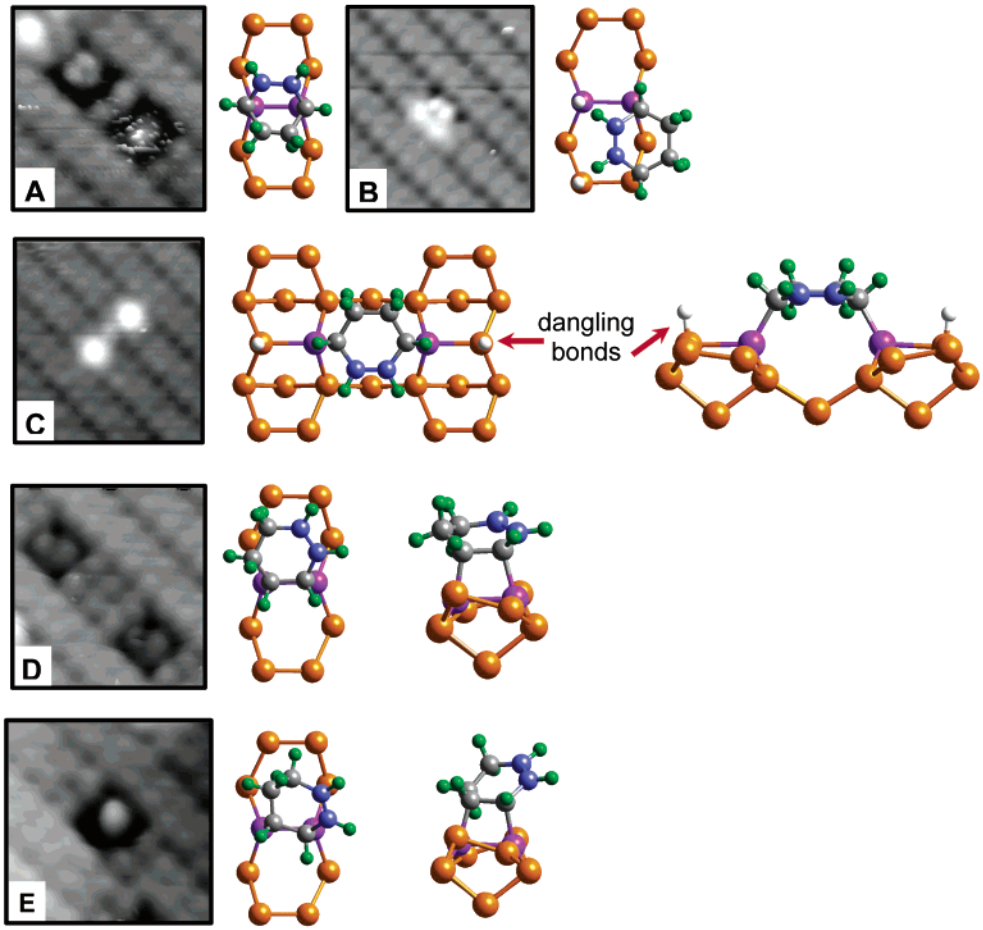

Figure 2. A−E show high-resolution STM images (~4 nm × 4 nm, $V_{tip} = -1.3$ V) and corresponding ball-and-stick models of the different reaction products. The models display overhead and side views of the attachment of 1,3-CHD (grey and green) to the underlying Si atoms (yellow). The Si dimer atoms bonded to the molecule are shown in purple, and the C═C that remains in the molecule after cycloaddition is shown in blue. Dangling bonds, shown in white, have been added in B and C for illustration only.

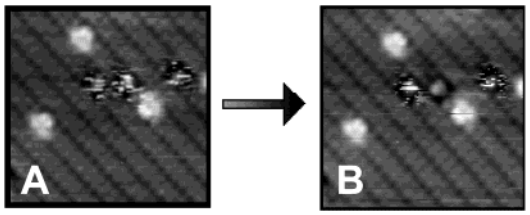

Figure 3. A and B are consecutive empty state images (7 nm × 7 nm, $V_{tip} = -1.3$ V) of the same area. In image B, one of the three unresolved features has decomposed into a recognizable product, which we identify as the [4 + 2]-like intradimer product.

the image and ball-and-stick model in Figure 2A reveals that the orientation and location of this maximum are consistent with the expected geometry of the intradimer [4 + 2] product.

Products B and C are [4 + 2]-like interdimer adducts due to the reaction of 1,3-CHD with Si atoms from two neighboring dimers. Reactions involving neighboring dimers within the same row result in the intrarow product B. The two unreacted Si dangling bonds (DBs) produced by this reaction appear as bright, well-separated maxima located to one side of the dimer row. The π orbital associated with the much shorter C═C bond in the 1,3-CHD adduct is also clearly seen and, as expected, is oriented along the dimer row direction (see Figure 2B). Reactions involving neighboring dimers in adjacent rows yield the inter-row product C. The molecule reacts with one Si atom from each dimer, and the "dumbbell" appearance is due to the two remaining unpaired Si DBs on either side of the reacted molecule. These DBs are located at the Fermi energy and dominate the image contrast.

The remaining products, D and E, are assigned to the two different conformers associated with a [2 + 2]-like intradimer reaction. Although previously unreported, their existence was predicted theoretically by Choi and Gordon.[8] In empty state images, both conformers have a two-dimer footprint similar to the intradimer [4 + 2] product (A). As in the case of A, images D and E should be interpretable in terms of the orientation of the C═C bond in the adduct. For conformer D, the plane of the C═C bond is roughly parallel to the surface whereas the bond itself is angled with respect to the dimer row direction. Because of this orientation, the STM tip is able to resolve two maxima, consistent with both the image and the schematic in Figure 2D. For conformer E, a single bright feature is observed that is offset to one side of the dimer row. However, in this case, the relaxed geometry in Figure 2E shows that the plane of the C═C bond is tilted up from the surface while the bond itself is located to one side of the dimer and oriented more or less along the dimer row direction. Consequently, a single maximum is typically observed. The location of this maximum is consistent with the geometry of conformer E.

We have not directly observed isomerization between the [2 + 2] conformers D and E at room temperature, despite the fact that Choi and Gordon calculated a barrier of only 0.39 eV. It is possible that conformers are artificially stabilized by the surrounding dimer structure in the same way buckled dimers are stabilized by the presence of surface defects. We have, however, observed streaky, fluxional features on the surface at room temperature following reaction with 1,3-CHD (see species F in Figure 1). At this juncture, it is not possible to establish whether these are rapidly isomerizing [2 + 2] products or some other species that is easily perturbed by the STM probe tip. While these species typically remain fluxional, we have occasionally observed decomposition into identifiable products. Figure 3 shows decomposition into the [4 + 2] intradimer product (species A).

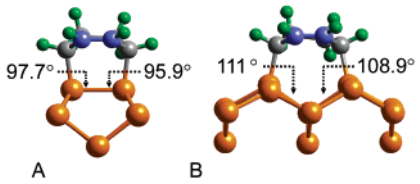

Figure 4. Ball-and-stick models in A and B show a side view of intra- and interdimer [4 + 2] reactions of 1,3-CHD with Si(100). The Si−C bond angles formed between the Si dimer atoms and the molecule are indicated.

TABLE 1: Relative Product Distribution of 1,3-CHD on Si(100)[16]

product	mode	%	product	mode	%
A	4 + 2	11 ± 3	D	2 + 2	10 ± 6
B	4 + 2	31 ± 6	E	2 + 2	12 ± 9
C	4 + 2	16 ± 7	F	?	21 ± 5

Table 1 provides an overview of the product distribution. In agreement with earlier studies, there is a pronounced preference for [4 + 2] attachment. This is not surprising since there is significant ring strain energy associated with the [2 + 2] attachment geometry. What is surprising, however, is that only 11% of the reactions are intradimer [4 + 2] reactions, whereas 31% are between two dimers in the same row, and 16% across rows. The interdimer species are predominant despite the fact that each involves the creation of two energetically unfavorable Si DBs. This clearly suggests that the ring strain is further relaxed by [4 + 2] attachment at the sites where the Si atoms involved in the reaction are farther apart than the 0.23 nm separation of the Si−Si dimer bond. However, our recent density functional theory (DFT) studies[12] have shown that the intradimer product A is thermodynamically favored and is 0.2 eV lower in energy than interdimer product B. Since it is well established that the creation of two unpaired DBs associated with product B costs between 0.3 and 0.5 eV,[15] the ring strain energy in the interdimer product B must be 0.1−0.3 eV lower than the intradimer product A. This suggestion is confirmed by a comparison of the attachment geometries for products A and B, which is shown in Figure 4. These schematics show the relaxed geometries from our total energy DFT calculations and clearly demonstrate that even though product A is lowest in energy there is a more significant departure from the preferred tetrahedral bonding geometry compared with product B.

Since the intradimer [4 + 2] product A is thermodynamically favored, the product distribution in Table 1 indicates that the reaction is kinetically controlled. Although the final state energies of the interdimer [4 + 2] products are higher due to the presence of the DBs, they are kinetically preferred because their attachment geometries involve less distortion of the incipient ring system in the transition state. Interconversion of these interdimer kinetic products to the thermodynamically favored intradimer [4 + 2] product is not possible due to the exceptional strength of the Si−C bonds formed.[8]

On the basis of these results, we can speculate on the nature of the reaction mechanism. The product distribution might simply reflect different barriers associated with the single step reaction pathways that lead to each product type. It is also plausible that attachment is a two-step radical reaction, with the initial step being the attachment of one end of the molecular π system to one of the Si dimer atoms. Figure 5 shows a schematic of this initial attachment geometry and demonstrates how subsequent reaction might account for the entire product distribution. Choi and Gordon[8] studied a structure similar to that in Figure 5 but identified it as a possible transition state

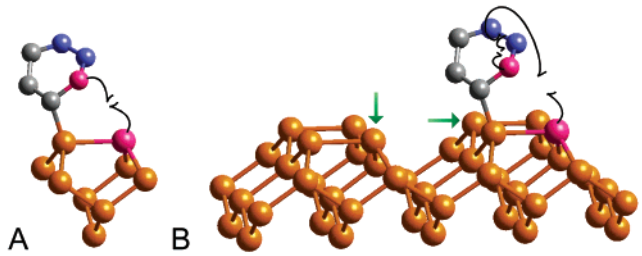

Figure 5. After the initial attachment of one end of the molecular π system in 1,3-CHD to the Si surface, all observed products can be formed following subsequent reaction. A and B show the [2 + 2] and [4 + 2] reaction possibilities, respectively. Atoms shown in pink are the Si and C radicals formed after initial attachment, and the C═C is shown in blue. Black arrows illustrate the movement of single electrons during reaction. In B, green arrows indicate Si atoms to which the final Si−C bond may also be formed to create the [4 + 2] interdimer products.

for the [2 + 2] reaction. The latter had an elongated Si−C bond and so was not a stable intermediate. However, it would seem that a relatively long-lived intermediate is required, one that is allowed sufficient time to sample all possible product channels. In contrast, a two-step ionic mechanism is inconsistent with the present results. Nucleophilic attack by the negatively charged up-atom of the Si dimer produces an allyl stabilized carbanion and a positively charged Si atom. While this ionic intermediate can, in principle, rearrange to produce the observed intradimer products (A, D, and E), formation of the interdimer products (B and C) requires efficient surface charge migration, which is unlikely due to the weakly dispersing bands[17] on this surface.

Conclusions

We have presented a high resolution STM study of the reaction of 1,3-CHD with Si(100). In addition to the intradimer [2 + 2] and [4 + 2] reaction products previously reported, two different [2 + 2] conformers are identified. Empty state STM images also show interdimer [4 + 2] reactions involving neighboring dimers in the same row and in adjacent rows. The former are shown to be the dominant surface product despite the presence of unpaired dangling bonds on two adjacent dimers. These results are interpreted in terms of a mechanism in which the reduced ring strain favors the kinetic interdimer [4 + 2] product over the thermodynamically stable [4 + 2] intradimer product. This interpretation is supported by fully relaxed DFT total energy calculations. The product distribution is consistent with a number of reaction mechanisms including the possibility of a single long-lived intermediate that undergoes subsequent reaction.

Acknowledgment. We would like to thank the National Science Foundation and the Science Foundation of Ireland for funding and the North Carolina Supercomputing Center for computational time.

References and Notes

(1) Hovis, J. S.; Liu, H.; Hamers, R. J. *J. Phys. Chem. B* **1998**, *102*, 6873.
(2) Wolkow, R. A. *Annu. Rev. Phys. Chem.* **1999**, *50*, 413.
(3) Teplyakov, A. V.; Kong, M. J.; Bent, S. F. *J. Am. Chem. Soc.* **1997**, *119*, 11100.
(4) Lopinski, G. P.; Fortier, T. M.; Moffatt, D. J.; Wolkow, R. A. *J. Vac. Sci. Technol., A* **1998**, *16* (3), 1037.
(5) Hovis, J. S.; Hamers, R. J. *Surf. Sci.* **1998**, *402−404*, 1.
(6) Padowitz, D. F.; Hamers, R. J. *J. Phys. Chem. B* **1998**, *102*, 8541.
(7) Konecny, R.; Doren, D. J. *J. Am Chem. Soc.* **1997**, *119*, 11098.
(8) Choi, C. H.; Gordon, M. S. *J. Am. Chem. Soc.* **1999**, *121*, 11311.
(9) Lopinski, G. P.; Wayner, D. D. M.; Wolkow, R. A. *Nature*, **2000**, *406*, 48. Bent, S. F. *Surf. Sci.* **2002**, *500*, 879, and references therein.
(10) Hamers, R. J.; Köhler, U. K. *J. Vac. Sci. Technol., A* **1989**, *7*, 2854.
(11) Kong, M. J.; Teplyakov, A. V.; Jagmohan, J.; Lyubovitsky, J. G.; Mui, C.; Bent, S. F. *J. Phys. Chem. B* **2000**, *104*, 3000.
(12) Computational details: Relaxation was performed using Cambridge Serial Total Energy Package (CASTEP). Milman, V.; Winkler, B.; White, J. A.; Pickard, C. J.; Payne, M. C.; Akhmatskaya, E. V.; Nobes, R. H. *Int. J. Quantum Chem.* **2000**, *77*, 895. In the full DFT slab calculations, slabs were six Si layers deep, with only the bottom two layers fixed at their bulk positions. Dangling bonds were terminated with hydrogen atoms and were also fixed. Each slab contained small supercells one dimer row wide and three dimers long, with the exception of geometry optimization of the inter-row species. For the electron exchange-correlation interaction, the generalized gradient approximation (GGA) functional was used with Perdew−Zunger parametrization: Perdew, J. P.; Zunger, A. *Phys. Rev. B* **1981**, *23*, 5048. Ultrasoft pseudopotentials were used for Si, C, and H atoms, and plane waves up to 230 eV were included in the basis set. Total energies calculated using the described parameters have an accuracy of ±5 meV.
(13) Mezhenny, S.; Lyubinetsky, I.; Choyke, W. J.; Wolkow, R. A.; Yates, J. T., Jr. *Chem. Phys. Lett.* **2001**, 344, 7.
(14) Hamaguchi, K.; Machida; Nagao, M.; Yasui, F.; Mukai, K.; Yamashita, Y.; Yoshinobu, J.; Kato, H. S.; Okuyama, H.; Kawai, M.; Sato, T.; Iwatsuki, M. *J. Phys. Chem. B* **2001**, *105*, 3718.
(15) Nachtigall, P.; Jordan, K. D.; Janda, K. C. *J. Chem. Phys.* **1991**, *95*, 8652.
(16) Error calculation based on analysis of 12 high-resolution images of ∼30 nm × 30 nm each.
(17) Chen, D.; Boland, J. J. *Phys. Rev. B* **2002**, *65*, 165336. †